JCTC Journal of Chemical Theory and Computation

Response of Scalar Fields and Hydrogen Bonding to Excited-State Molecular Solvation of Carbonyl Compounds

Anant D. Kulkarni,* Benedetta Mennucci,* and Jacopo Tomasi

Dipartimento di Chimica e Chimica Industriale, Università di Pisa, Via Risorgimento 35, 56126 Pisa, Italy

Received September 21, 2007

Abstract: An attempt has been made to understand the mechanism of excited-state molecular solvation and its effect on hydrogen bonding in carbonyl compounds in aqueous solution. The correlation between solvation and electronic transitions has been investigated by comparing results obtained either with a supermolecular description in terms of hydrogen-bonded clusters or with a combined method embedding such clusters with a polarizable continuum dielectric mimicking the bulk water. Popular scalar fields such as molecular electrostatic potential and molecular electron density have been used as useful tools to probe the changes in the hydrogen bonding passing from ground to excited states in the gas as well as solvent phase.

1. Introduction

Water is the omnipresent solvent in almost all important chemical and biological processes. Thus, it is no wonder that the study of molecular hydration, dealing with the interaction of water with other molecules, has become an area of prime importance in chemistry and biology.[1,2] The hydration of molecules containing a carbonyl group has been the focus of several studies.[3–15] In particular, the carbonyl double bond shows spectroscopically important transitions such as $n \rightarrow \pi^*$ and $\pi \rightarrow \pi^*$, which are well-known examples of environment-sensitive processes. Two prototype examples of molecules containing carbonyl groups, namely, formaldehyde (H_2CO) and urea ($CO(NH_2)_2$), are considered in the present study.

The earlier studies on formaldehyde and water (in the ground state) complexes at the HF level were reported by Tomasi and co-workers[5a] with reference to the environmental effects on biomolecules, followed by yet another *ab initio* study[5b] discussing the solvent shift of electron absorption spectra. Later on, 1:1 complexes of formaldehyde···water systems were studied at the MPn[6a,b] and CCSD level.[6c] Wolfe et al.[7] performed *ab initio* calculations on the hydration of formaldehyde with up to four water molecules and reported the thermochemical parameters and vibrational frequencies. More recently, combined quantum mechanics/molecular mechanics approaches have been used to calculate molecular response properties and excitation energies of formaldehyde in water.[8]

The water-soluble nature of urea is well-known. The effect of the molecular environment on the optical susceptibility of urea in solution has been studied by Ledoux and Zyss.[9] According to the earlier studies[10] based on MD simulations, the urea molecule can enter the cluster of water molecules without appreciable distortion in the hydrogen-bonded network of water molecules. A clear conclusion about the hydrophobic or hydrophilic nature of urea could not be drawn from this work. A detailed study addressing the solvent and the vibrational effect on static and dynamic polarizabilty as well as hyperpolarizability within the quantum chemical framework has been reported by our group.[11] Lee et al.[12] performed density functional theory (DFT) computations on the complexes between urea, water, and urea dimers, using VWN and BLYP functionals and DZ94 and DZ94P basis sets. According to this study, the urea dimer will be unstable due to the interaction between the urea and water molecules when surrounded by a large number of water molecules. Åstrand and co-workers[13] employed the empirical-potential-based as well as the quantum-chemical approach to study urea···water complexes. The most favorable structure for the urea···water complex has two hydrogen bonds and is cyclic in nature.

* Corresponding author. E-mail: anantkul@dcci.unipi.it and anantkul@chem.unipune.ernet.in (A.D.K.), bene@dcci.unipi.it.

10.1021/ct7002429 CCC: $40.75
Published on Web 02/29/2008

Following this historical summary, a brief preamble to the scalar-field-based studies is useful since this study involves the extensive use of popular scalar fields, namely, molecular electrostatic potential (MESP, also denoted by V_{es}) and molecular electron density (MED also denoted by $\rho(\mathbf{r})$).

Bader and co-workers pioneered the topographical studies of MED.[16] Also, Gatti and co-workers[17] performed extensive studies involving molecular electron-density-based approaches. The use of MESP as a useful tool to predict the molecular properties was first advocated by Scrocco and Tomasi[18a] more than 3 decades ago. Tomasi and co-workers[18b] have summarized the applications of MESP for studying the intermolecular interactions in great detail by highlighting the important aspects of molecular structure and solvation effects. Politzer and Thruhlar[19] have also advocated the utility of a MESP-based approach through various studies. Extensive topographical investigations of MED and MESP have been carried out by Gadre and co-workers[20–22] to understand hydrogen-bonded interactions over the past decade or so.

In view of this, it is worthwhile to study the excited-state molecular solvation process and the corresponding spectroscopic properties and to probe the correlation between this process and hydrogen-bonding interactions using MESP and MED, the popular scalar fields. In particular, the following questions will be addressed:

What is the effect of an electronic excitation on the hydrogen bonding of explicitly bound water molecules in the ground state?

Can one use the information from scalar fields such as MESP and MED to understand this process?

What are the effects on this process due to the solvent, treated as an external, continuous medium, thereby taking into account the bulk solvation effect?

The present paper is organized as follows: section 2 deals with methodological aspects employed, and the results and discussion are presented in section 3, where numerical results are presented and discussed. Section 4 concludes the article and also presents future extensions of the present study.

2. Methodology

The structures of M···H_2O clusters (where M = formaldehyde and urea) were generated from the knowledge of earlier studies[6,22] (both in the gas and solution phases) and the cooperativity offered by MESP.[20–22] The geometry optimizations for the ground and excited states, in the gaseous state as well as in the solution (water) state, were achieved with the Gaussian program package.[23] The ground states were first obtained at the HF/6-31G(d,p) level, whereas the excited-state geometries were computed employing the simple *ab initio* configuration interaction, including only single excited configurations (CIS).

In order to enhance the level of sophistication, we have also employed DFT. Application of DFT-based methods in studying hydrogen-bonded complexes could be a question of debate. However, the success of using a DFT approach for studying hydrogen-bonded interactions has been highlighted by several researchers.[24] The popularity of these methods may be attributed to the fact that they model the exchange correlation effects, at a considerably lower computational cost than other correlated methods.[24] As highlighted by Dreuw and Head-Gordon,[25] time-dependent DFT (TD-DFT) has emerged as a reliable and prominent method to study the excited-state properties of medium- and large-sized molecular systems. Also, the earlier studies,[26,27] by other researchers and by one of the present authors, have demonstrated the reliability of TD-DFT-based methods for studying the excited states. Taking a cue from these studies, we have used the B3LYP functional, which is a combination of Becke's three-parameter functional[28] with the correlation functional of Lee, Yang, and Parr.[29] In order to increase the level of sophistication, we have employed a split valence triple-ζ basis set augmented with a diffuse and polarization function, 6-311++G(d,p), along with the time-independent and time-dependent versions of density functional theory using B3LYP and TD B3LYP frameworks[30,31] for ground- and excited-state properties, respectively. The extended basis set employed in this work, that is, 6-311++G(d,p), has been used in the (6d) version as implemented in Gaussian.[23] The molecular orbitals were visualized using GVIEW,[32] to follow the electronic transitions.

2.1. Solvation Study. The present study employs the integral equation formalism−polarizable continuum model (*IEF-PCM*) solvation model,[33] an accurate reformulation of the PCM model[34] due to Tomasi and co-workers. The IEF-PCM model involves mimicking the solvent in a dielectric continuum fashion with a dielectric constant (ϵ) which surrounds the molecular cavity, with the shape and dimension adjusted on the real geometric structure of the solute molecule. The latter polarizes the solvent and induces an electric field (the "reaction field") that interacts with the solute. In the IEF-PCM model, the solute–solvent electrostatic interaction is represented in terms of an apparent charge density spreading on the cavity surface, giving rise to specific operators which contribute to the Hamiltonian of the isolated system (to obtain the final effective Hamiltonian). Such solvent terms depend on the solute wave function they contribute to modify, and thus, the problem requires the solution of a modified self-consistent field scheme.

In general, the solute electronic and nuclear charge distribution and solvent reaction field are allowed to mutually equilibrate. However, when the solute undergoes an abrupt change of its electronic state through a vertical transition, the relaxation of the reaction field in the direction of the new solute state may be incomplete (nonequilibrium solvation). Considering the typical time scales characterizing electronic and nuclear (or molecular) motions, we assume that only the part of the solvent reaction which is induced by the polarization of its electrons can immediately be modified according to the new electronic state, which is reached by the solute in the transition process. The other part in the system remains frozen under the previous equilibrium conditions as determined by the initial state. In a reasonable approximation, the fast component can be taken proportional to the dielectric constant at infinite frequency ϵ_∞ where $\epsilon_\infty \approx n^2$ and n is the refractive index of the solvent. In IEF-PCM framework, this scheme is implemented by introducing two sets of apparent charges representing the

electronic (or fast) and the slow contributions of the solvent reaction. IEF-PCM has been generalized to CIS and TD-DFT calculations which also include solvent perturbation operators in the coupled perturbed scheme; for more details on the formalism, see refs 35 and 36. The values used in the following calculations for the ϵ and ϵ_∞ of water are 78.39 and 1.776, respectively.

2.2. MESP and MED Analysis and Visualization. The present work involves extensive use of MESP and MED and their topographical analysis in terms of critical points (CPs). The CPs provide valuable information about the structure, bonding features, and environment of the molecule. The details of electrostatic potential, electron density, topography, and related concepts may be found elsewhere.[14,16,20,21] MESP and MED over the regular grids enclosing the molecular system under study were computed using the Gaussian package.[23] The topographical analysis for various electronic states was performed by following the MOs for each specific transition and the density matrices computed at respective levels employing the UNIPROP[37] and UNIVIS-2000[38] packages. In the present study, we have employed the information provided by (3, −1) MESP and MED CPs computed in the bonding region between the two molecules. The Laplacian of the electronic density ($\nabla^2\rho(\mathbf{r})$) has also been used to understand the bonding features in this study.[16] The negative value of $\nabla^2\rho(\mathbf{r})$ implies a preponderance of electron density and hence is an indicator of a covalent bond, whereas its positive value indicates nonbonding or closed-shell interaction such as hydrogen bonds between the two atoms.[16–20] The geometry generation and visualization of scalar fields were carried out with the help of the versatile visualization package, UNIVIS-2000.[38]

3. Results and Discussion

The results of the quantum chemical investigation of the effects of H bonds on excited states in terms of a combined molecular solvation approach (i.e., a supermolecular description involving hydrogen-bonding effects and the bulk effects as represented by a continuum solvation) are discussed as follows.

The analysis is focused on $n-\pi^*$ excited states of the gas phase and solvated M···H_2O clusters studied at the HF/6−31G(d,p) and CIS/6–31G(d,p) levels (referred to as level I); B3LYP/6−311++G(d,p) and TDB3LYP/6−311++G(d,p) (referred to as level II). The additional results for $\pi \rightarrow \pi^*$ transitions are also reported as a comparison.

In order to probe the geometrical and energetic changes in the excited-state formation/relaxation, we consider the excitation process to occur via a stepwise mechanism. In the gas phase, such a mechanism is clear: a relaxed ground state is first vertically excited into a Franck–Condon (FC) (i.e., geometrically unrelaxed) excited state, which then relaxes into a completely equilibrated excited state.

As discussed in section 2.1., in solution, the picture is more difficult as two different solvation regimes have to be considered when fast modifications in the solute occur. Here, these two regimes give rise to the following process: initially an equilibrated ground state is vertically excited into a FC state embedded in a nonequilibrated solvent (step 1); successively, the solvent relaxes toward an equilibrium regime with respect to the FC state (step 2), and finally both the solute and solvent reach a completely relaxed state (step 3). This schematization assumes that solvent dielectric relaxation proceeds faster than the solute geometrical relaxation. An alternative approach would be that of deleting step 2 and assuming that solute and solvent relaxations proceed contemporaneously. Both of these approaches are clearly approximations of the real process, but they are useful in the present context as they provide insights about solvation effects on excited-state formation and relaxation.

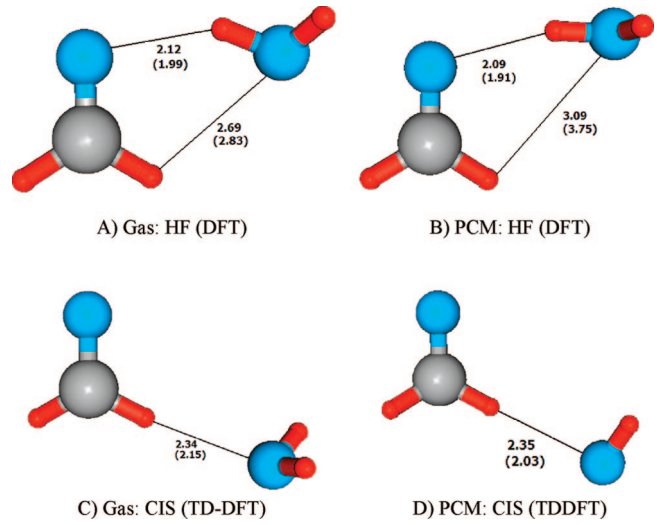

Figure 1. Schematic representation of gas- and solvent-phase structures of ground (A and B) and $n-\pi^*$ excited (C and D) states of *formaldehyde···water* complexes at HF-CIS and DFT−TD-DFT levels. All of the distances are in angstroms, and the values in parentheses indicate the distances computed at the B3LYP/6−311++G(d,p) level of theory. Refer to the text for details.

Figures 1 and 2 present the schematic representation of the most stable structures obtained for the ground and relaxed $n-\pi^*$ excited states at level I and level II for the gas and solvent phases, whereas in Table 1, we report the corresponding vertical excitation energies (for level I $\pi-\pi^*$, data are also reported).

3.1. Gas-Phase H-Bonded Clusters. For both systems, a cyclic structure with two hydrogen bonds is found in the ground state, while the geometrical relaxation of the excited state results in overall modification of the hydrogen-bonding picture by pushing the water molecule away from the carbonyl oxygen (toward the hydrogen of formaldehyde and urea). Going into a more detailed comparison between the two systems, we find that H-bond distances are shorter in urea both for the CO···HOH in the ground state and the H···OH_2 in the relaxed excited state. Such a picture does not change passing from one to the other level of calculations. However, DFT computations predict a shortening of the hydrogen-bond lengths for both the ground and the relaxed excited states.

Moving to the absorption process, it may be seen from Table 1 that the vertical excitation energies for $n \rightarrow \pi^*$ transitions are always lower than the corresponding $\pi \rightarrow \pi^*$ transitions. Also, TD-DFT results are comparatively lower than their

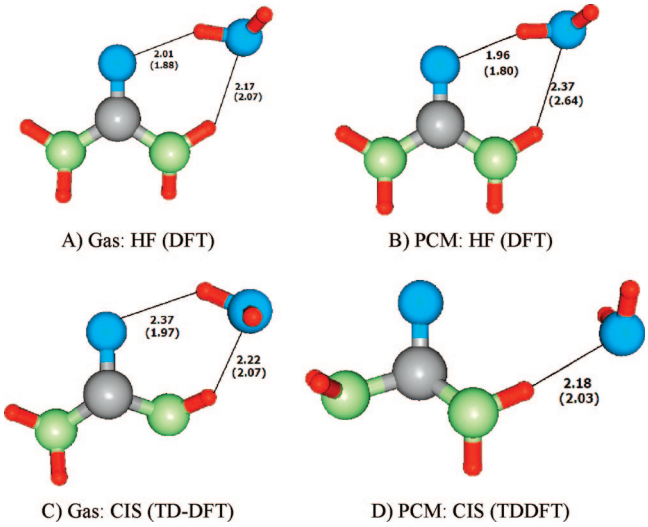

Figure 2. Schematic representation of gas- and solvent-phase structures of ground (A and B) and $n-\pi^*$ excited (C and D) states of *urea···water* complexes at HF-CIS and DFT−TD-DFT levels. All of the distances are in angstroms, and the values in parentheses indicate the distances computed at the B3LYP/6−311++G(d,p) level of theory. Refer to the text for details.

Table 1. Excitation Energies ($n \rightarrow \pi^*$ and $\pi \rightarrow \pi^*$ Transitions) for M···H_2O Clusters (M = Formaldehyde and Urea) in the Gas Phase and in Water[a]

		level I[b]		level II[c]
molecular system	gas/solvent	$n \rightarrow \pi^*$	$\pi \rightarrow \pi^*$	$n \rightarrow \pi^*$
formaldehyde···H_2O	gas	4.91	10.57	4.09
	water	5.02	10.50	4.17
urea···H_2O	gas	8.36	9.97	7.17
	water	8.77	10.35	7.27

[a] Excitation energies are in electrovolts. [b] CIS/6-31G(d,p) level. [c] TD B3LYP/6−311++G(2d,2p) level. (Refer to the text for further details.)

corresponding values at the CIS level toward a better agreement with experiments (see below). Here, however, it is more interesting to quantify the effect of the H bonds as described by the two levels of calculations.

In $n \rightarrow \pi^*$ transitions, the electronic density on the heteroatom (here, the carbonyl oxygen) decreases upon excitation. As a result, the tendency of the heteroatom to form hydrogen bonds is reduced with respect to the ground state. Introducing the effect of the H-bonded water should thus lead to higher absorption energy (i.e., a blue-shift), and the stronger the hydrogen bond is, the larger is the shift.

To verify this picture, we have optimized the structures of isolated (i.e., in the absence of H-bonded water) formaldehyde and urea and calculated the $n-\pi^*$ excitation energies (this analysis has been limited to level I). The results obtained are 4.73 and 7.79 eV for formaldehyde and urea, respectively; by combining these results with the data reported in Table 1 for the gas-phase M···H_2O clusters, we obtain blue-shifts of 0.18 and 0.57 eV for formaldehyde and urea, respectively.

Correlating these shifts with the H-bond distances reported in Figures 2 and 3, it may be seen that our computations perfectly reproduce the criterion which is generally used in

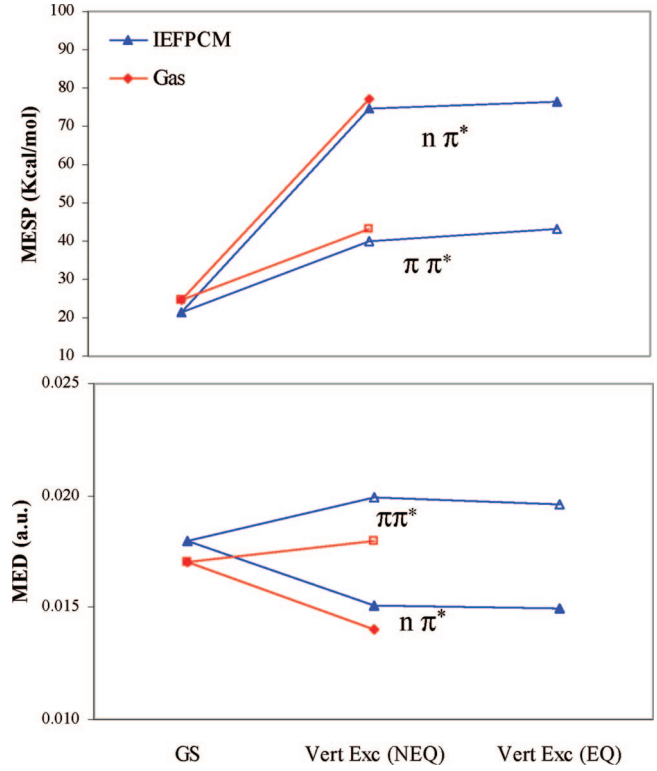

Figure 3. MESP (upper panel) and MED (lower panel) values for formaldehyde···H_2O clusters at the RHF-CIS/6−31G(d,p) level in the ground and vertical excited states ($n\pi^*$ and $\pi\pi^*$) in the gas phase and in water. For the solvated systems, two vertical excited states are reported corresponding to nonequilibrium and equilibrium solvation, respectively.

the analysis of the shift in the $n \rightarrow \pi^*$ band for determining the energy of the hydrogen bond.

The $\pi \rightarrow \pi^*$ transitions show an altogether different behavior as compared to that exhibited by $n \rightarrow \pi^*$. In case of these transitions, it is generally observed that the heteroatom is more basic in the excited state than in the ground state. The resulting excited molecule thus involves a stronger hydrogen bond as compared to the ground state, and a red-shift is expected for the excitation energies.

As a result of this, we expect the clusters with stronger H bonds to give smaller transition energies (i.e., larger red-shifts). By comparing $\pi \rightarrow \pi^*$ transition energies of the isolated formaldehyde and urea (10.58 and 10.09 eV) with those reported in the table for the M···H_2O systems, we see that, once again, the predicted behavior is confirmed by the calculations in which urea shows the largest red-shift.

3.2. Solvated H-Bond Clusters. A look at the Figures 1 and 2 reveals that the solvent effect as incorporated by IEF-PCM leads to a shortening of (C)O···H(OH) hydrogen bonds for the ground states of both systems at both levels of calculations. This shortening indicates strengthening of the H bond due to the effects of the additional water molecules (here, represented by the polarizable continuum dielectric).

In the case of the completely relaxed excited states, we observe structures with a nonplanar solute and only one hydrogen bond, similarly to what was found in the gas phase. The larger urea···H_2O system presents a larger nonplanarity due to rotation around the C−N bond. This change may be

regarded as a signature of solvation in terms of structural deformation.

The differences in the geometrical structures of ground and excited states passing from the gas phase to solvated clusters are reflected in the shifts in the excitation energies. The introduction of the continuum solvent leads to a significant blue-shift for $n \rightarrow \pi^*$ transitions and a smaller red-shift for $\pi \rightarrow \pi^*$ transitions. This result can be better explained considering in more details all of the possible effects that the solvent has on the absorption process.

In the previous section, we quantified the effect of H bonds on the $n \rightarrow \pi^*$ transition in terms of the blue-shifts with respect to the isolated molecule. Here, we can extend such an analysis by adding the effect of all the other solvent molecules (i.e., the bulk of the solvent). Such a bulk effect acts in a 2-fold way: it modifies the structure of the H-bonded clusters, as commented above, and it directly affects the ground and excited states by differentially stabilizing them. As a result of these two effects, the excitation energies will be changed with respect to the gas-phase clusters. From Table 1, we see that the net bulk effect leads to further blue-shifts of 0.11 and 0.41 eV for formaldehyde and urea at level I (this picture remains consistent at level II but with smaller shifts).

At this stage it is felt worthwhile to dissect these shifts in terms of their (structural and direct) components. This is easily obtained by recalculating the excitation energies of the solvated clusters but, this time, keeping their structure fixed in the gas-phase geometry. The results obtained are 5.08 and 8.69 eV for formaldehyde and urea, respectively; these data when compared with the corresponding ones reported in Table 1 (namely, 5.08 and 8.77 eV) show that the effects the bulk solvent has on the geometry of the H-bonded systems (and indirectly on the excitation energies) are negligible for formaldehyde, whereas they lead to a further blue-shift (of 0.08 eV) for urea.

The $\pi \rightarrow \pi^*$ transitions show an altogether different behavior as compared to that exhibited by $n \rightarrow \pi^*$. In case of these transitions, we have previously observed that the heteroatom is more basic in the excited state than in the ground state. The resulting excited molecule thus involves a stronger hydrogen bond as compared to the ground state, and as a result, a red-shift on the absorption of the cluster is found with respect to the isolated molecule. Within this picture, the addition of the bulk effects should induce a further red-shift: this is confirmed by our calculations in which IEF-PCM $\pi \rightarrow \pi^*$ energies are always smaller than the corresponding ones calculated in the gas-phase clusters.

Even if the present work is not primarily aimed at a comparison with experiments, it is useful to conclude this analysis with some information on the observed spectra of these compounds. Although the pure electronic $n-\pi^*$ transition of formaldehyde is forbidden, a band due to the coupling with vibrational modes mainly involving the out-of-plane bending motion is observed in the experiments.[38] The experimental value[38] for the gas phase is 3.5–4.0 eV. An experimental value of the blue-shift for monomeric formaldehyde in water is not available due to

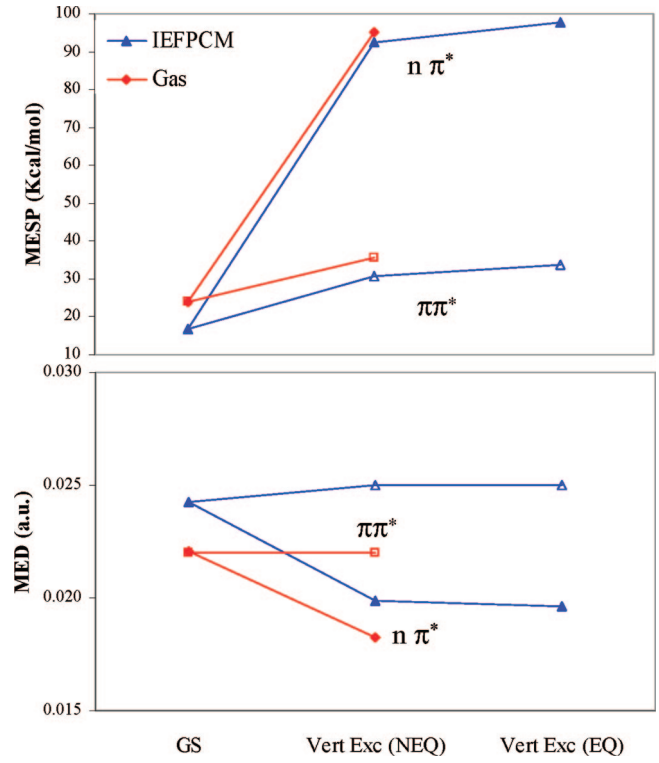

Figure 4. MESP (upper panel) and MED (lower panel) values for urea···H_2O clusters at the RHF-CIS/6−31G(d,p) level in the ground and vertical excited states ($n\pi^*$ and $\pi\pi^*$) in the gas phase and in water. For the solvated systems, two vertical excited states are reported corresponding to nonequlibrium and equilibrium solvation, respectively.

the formation of oligomers. However, it is likely to be around 0.23 eV, the value observed for acetone. The results reported in Table 1 when compared to the values of the free molecule in the gas phase (4.73 eV at level I and 3.96 eV at level II) lead to shifts on the order of 0.16 eV (level I) and 0.13 eV (level II) for the isolated supermolecule and 0.26 eV (level I) and 0.21 eV (level II) for the solvated (IEF-PCM) one.

To the best of our knowledge, UV absorption spectra of urea have not been investigated in depth, and the electronic transitions of the urea chromophore have not been determined either experimentally or theoretically.

3.3. MESP and MED Analysis. Figures 3 and 4 depict the graphical comparison of the MESP and MED values for $n \rightarrow \pi^*$ and $\pi \rightarrow \pi^*$ (the electrostatic potential values in the graphs are converted into kcal/mol counterparts) in the gas phase and in solution. The details of the $n \rightarrow \pi^*$ transition for the gas phase and solvent phase are summarized in Tables 2 and 3, respectively.

The variation of MESP plotted in a plane containing the molecular system and hydrogen bonds is finally depicted in Figure 5 for solvated clusters at the ground, vertical excitation, and completely relaxed $n-\pi^*$ excited states. The positive-valued electrostatic potential is indicated by the red color and the negative valued potential by blue. The white region between the molecules stands for the small or zero-valued potential value or bonding region of the cluster.

The trends in the MESP and MED for formaldehyde···H_2O and urea···H_2O complexes are qualitatively similar. The $-NH_2$

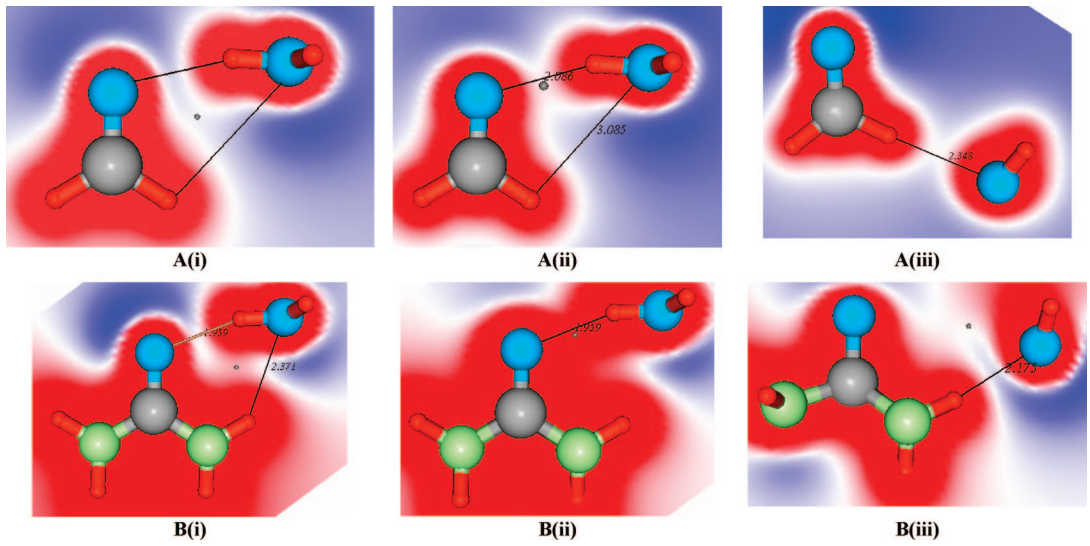

Figure 5. Schematic representation of structures and MESP mapped on the planes containing molecules and hydrogen bonds computed for (A) formaldehyde···H_2O and (B) urea···H_2O complexes at the RHF-CIS/6−31G(d,p) level in the (i) ground state (solvent), (ii) vertical excitation state (solvent), and (iii) fully relaxed excited states (solvent).

Table 2. Details of MESP and MED Critical Points (3, −1) for $n \rightarrow \pi^*$ Transition of M···H_2O clusters (M = Formaldehyde and Urea) in the Gas Phase[a]

	level I			level II		
	ground state	vertical exc. state	relaxed exc. state	ground state	vertical exc. state	relaxed exc. state
			(A) Formaldehyde···Water Complex			
MESP	0.039	0.123	0.039	0.069	0.157	0.007
$\rho(\mathbf{r})$	0.017	0.014	0.012	0.023	0.019	0.016
$\nabla^2\rho(\mathbf{r})$	0.057	0.053	0.037	0.082	0.077	0.057
			(B) Urea···Water Complex			
MESP	0.038	0.151	0.029	0.063	0.225	0.069
$\rho(\mathbf{r})$	0.016	0.017	0.007	0.026	0.027	0.024
	0.022	0.018	0.015			
$\nabla^2\rho(\mathbf{r})$	0.071	0.065	0.049	0.103	0.107	0.085

[a] MESP and MED values at the CPs are in atomic units (au). Level I: CIS/6−31G(d,p). Level II: TD B3LYP/6−311++G(2d,2p). (Refer text for further details.)

Table 3. Details of MESP and MED Critical Points (3, −1) for $n \rightarrow \pi^*$ Transition of M···H_2O Clusters (M = Formaldehyde and Urea) in Water[a]

	level I				level II			
	ground state	vertical exc. state (NEQ)	vertical exc. state (EQ)	relaxed exc. state	ground state	vertical exc. state (NEQ)	vertical exc. state (EQ)	relaxed exc. state
				(A) Formaldehyde···Water Complex				
MESP	0.034	0.119	0.122	0.025	0.069	0.150	0.155	0.035
$\rho(\mathbf{r})$	0.018	0.015	0.015	0.015	0.026	0.023	0.023	0.023
$\nabla^2\rho(\mathbf{r})$	0.056	0.052	0.052	0.035	0.095	0.094	0.095	0.074
				(B) Urea···Water Complex				
MESP	0.027	0.148	0.156	−0.009	0.059	0.106	0.115	0.009
$\rho(\mathbf{r})$	0.024	0.019	0.019	0.017	0.035	0.035	0.035	0.019
$\nabla^2\rho(\mathbf{r})$	0.077	0.070	0.070	0.048	0.117	0.122	0.120	0.069

[a] MESP and MED values at the CPs are in atomic units (au). Level I: CIS/6−31G(d,p). Level II: TD B3LYP/6−311++G(2d,2p). (Refer text for further details.)

groups in the case of urea have marginal effects on the hydrogen-bond-forming ability. The results in Figures 2 and 3 indicate that the MESP CP becomes more positive on $n \rightarrow \pi^*$ excitation, whereas for $\pi \rightarrow \pi^*$ vertical transition, this change is rather small due to marginal perturbation in the H-bonding environment. In the case of electron density, the $n \rightarrow \pi^*$ excitation show a decrease in the transition from the ground to the vertical excited state but only a very small increase for the $\pi \rightarrow \pi^*$ transition.

In general, it may be noticed that the CP values computed within the DFT framework (level II) are higher than their counterparts within the HF framework (level I). The reason for the differences in the absolute values may be attributed to the difference in the molecular geometries at the HF and DFT/B3LYP levels. In the case of the DFT level, the proton of H_2O was pulled more toward the carbonyl oxygen, and the angle of approach has been found to be larger at the HF level (see Figures 1 and 2).

The inclusion of the external IEF-PCM continuum does not change the qualitative behavior of MESP and MED values observed in the gas phase, but it affects the absolute values.

In greater detail, the first step of the excitation process (namely, the vertical excitation with a nonequilibrium solvent) presents the same features observed in the gas phase: MESP values at a CP increase of ~3–4 times with respect to the ground-state value for level I (and ~2 times for level II). These CP values show a further small increment when solvent is allowed to become equilibrated. Once again, the final relaxation of the solute geometry (in equilibrium with the solvent) is accompanied by a significant reduction of the MESP to a value nearly close to the ground-state one. The sudden modification of electrostatic potential values while going from the ground state to different excited states was reported previously by Shukla and Leszczynski,[27b] whereas preliminary analyses on the effects of excitations on MESP were given by Tomasi and co-workers more than 3 decades ago.[41]

As a final analysis, let us consider $\nabla^2\rho(\mathbf{r})$ values evaluated at the MED CP (see Tables 2 and 3). We recall that negative values of $\nabla^2\rho(\mathbf{r})$ at the MED CP have been used as an indication of a covalent bond, whereas positives value are an indicator of noncovalent or hydrogen-bonded character. From the results reported in Tables 1 and 2, we have confirmation of this indication: $\nabla^2\rho(\mathbf{r})$ values evaluated at the MED CP are all positive for both systems either in the gas phase or in water. However, for this property, the effect of excitation is rather small.

4. Summary

This article presents an investigation on the correlation between hydration effects and $n \rightarrow \pi^*$ and $\pi \rightarrow \pi^*$ excitation processes in carbonyl compounds.

In such an analysis, two different models have been compared, one using gas-phase H-bonded clusters and the other using H-bonded clusters plus an external continuum solvation (IEF-PCM). To describe the formation/relaxation of the excited state, a different stepwise mechanism is introduced in both models. For the gas phase, the standard picture in terms of a two-step process passing through the Franck–Condon state is used, while for IEF-PCM solvated clusters, a further intermediate step corresponding to solvent dielectric relaxation in succession to the vertical excitation is added to include bulk water effects. The changes in geometries and energetics of the ground and excited states have been analyzed using two popular scalar fields, that is, the molecular electrostatic potential and the molecular electron density.

The MESP CPs show a drastic increase (about 2–3 fold with respect to the ground state) upon first excitation, and this remains fairly similar when solvent relaxation is considered. However, solvent equilibrium along with the complete geometrical relaxation leads to a stabilization of the MESP value close to the ground-state value. A different behavior is found for MED, for which a significant decrease is observed for $n \rightarrow \pi^*$ transitions and a minor increase for $\pi \rightarrow \pi^*$ transitions. These trends in the scalar fields may be attributed to structural distortions in the planarity of the molecule and in the modification of the hydrogen-bond network. By contrast, the Laplacian of electron density, $\nabla^2\rho(\mathbf{r})$, values show very subtle changes after excitation. Hence, the information from $\nabla^2\rho(\mathbf{r})$ seems not to be usefully exploited to draw any specific conclusion about possible correlations between hydrogen bonds, bulk effects, and electronic excitations.

It is expected that more studies based on a similar approach for different carbonyl compounds are necessary to generalize the conclusions. Further studies on a similar theme are underway in our laboratory.

Acknowledgment. A.D.K. is thankful to Professors Shridhar R. Gadre, Rajeev K. Pathak (University of Pune, Pune, India) and Carlo Gatti (CNR-ISTM, Milan, Italy) for useful discussions and suggestions. The authors acknowledge the financial support of Gaussian Inc.

References

(1) Jeffrey, G. A. *An Introduction to Hydrogen Bonding*; Oxford: New York, 1997.

(2) Desiraju, G. R.; Steiner, T. *The Weak Hydrogen Bond*; Oxford: New York, 1999.

(3) Lewell, X. Q.; Hillier, I. H.; Field, M. J.; Morris, J. J.; Taylor, P. J. *J. Chem. Soc., Faraday Trans.* **1988**, *84*, 893.

(4) Cai, Z.; Reimers, J. R. *J. Phys. Chem. A* **2007**, *111*, 954.

(5) (a) Alagona, G.; Pullman, A.; Scrocco, E.; Tomasi, J. *Int. J. Peptide Protein Res.* **1973**, *5*, 251. (b) Cimiraglia, R.; Miertus, S.; Tomasi, J. *Chem. Phys. Lett.* **1981**, *80*, 286.

(6) (a) Kumpf, R. A.; Damewood, J. R., Jr. *J. Phys. Chem.* **1989**, *93*, 4478. (b) Dimitrova, R. A.; Peyerimhoff, G. D. *J. Phys. Chem.* **1993**, *97*, 12731. (c) Ramelot, T. A.; Hu, C.-H.; Fowler, J. E.; Deleeuw, B. J.; Schaefer, H. F. *J. Chem. Phys.* **1994**, *100*, 4347.

(7) Wolfe, S.; Kim, C.; Yang, K.; Weinberg, N.; Shi, Z. *J. Am. Chem. Soc.* **1995**, *117*, 4240.

(8) (a) Canuto, S.; Coutinho, K. *Int. J. Quantum Chem.* **2000**, *77*, 192. (b) Kawashima, Y.; Dupuis, M.; Hirao, K. *J. Chem. Phys.* **2002**, *117*, 248. (c) Kongsted, J.; Osted, A.; Pedersen, T. B.; Mikkelsen, K. V.; Christiansen, O. *J. Phys. Chem. A* **2004**, *108*, 8624.

(9) Ledoux, I.; Zyss, J. *Chem. Phys.* **1982**, *73*, 203.

(10) Tanaka, H.; Touhara, H.; Nakanishi, K.; Watanabe, N. *J. Chem. Phys.* **1984**, *80*, 5170.

(11) Mennucci, B; Cammi, R.; Cossi, M.; Tomasi, J. *THEOCHEM* **1989**, *426*, 191.

(12) Lee, C.; Stahlberg, E. A.; Fitzgerald, G. *J. Phys. Chem.* **1995**, *99*, 17737.

(13) Åstrand, P.-O.; Wallqvist, A.; Karlström, G.; Linse, P. *J. Chem. Phys.* **1991**, *95*, 8419.

(14) (a) Wolfe, S.; Kim, C.; Yang, K.; Weinberg, N.; Shi, Z. *J. Am. Chem. Soc.* **1995**, *117*, 4240. (b) Sivanesan, D.; Subramaniam, V.; Babu, K.; Gadre, S. R. *J. Phys. Chem. A* **2000**, *104*, 10887. and the references therein. (c) Shishkin, O. V.; Gorb, L.; Leszczynski, J. *J. Phys. Chem. B* **2000**, *104*, 5357. (d) Kim, N. J.; Kang, H.; Jeong, G.; Kim, Y. S.; Lee, K. T.; Kim, S. K. *J. Phys. Chem. A.* **2000**, *104*, 6552.

(15) (a) Kim, S.; Wheeler, S. E.; Schaefer, H. *J. Chem. Phys.* **2006**, *124*, 204310. (b) Kim, N. J. *Bull. Korean Chem. Soc.* **2006**,

27, 1009. (c) Schiedt, J.; Weinkauf, R.; Neumark, D. M.; Schlag, E. W. *Chem. Phys.* **1998**, *239*, 511. (d) Li, X.; Cai, Z.; Sevilla, M. D. *J. Phys. Chem. A* **2002**, *106*, 1596. (e) Pal, S. K.; Peon, J.; Zewail, A. H. *Chem. Phys. Lett.* **2002**, *363*, 57.

(16) (a) Bader, R. F. W. *Atoms in Molecules - A Quantum Theory*; Oxford University Press: Oxford, 1990. (b) Bader, R. F. W.; Essen, H. *J. Chem. Phys.* **1984**, *80*, 1943. (c) Bone, R. G. A.; Bader, R. F. W. *J. Phys. Chem.* **1996**, *100*, 10892.

(17) Gatti, C; May, E.; Destro, R.; Cargnoni, F. *J. Phys. Chem. A* **2002**, *106*, 2607. and the references therein.

(18) (a) Scrocco, E.; Tomasi, J. *Top. Curr. Chem.* **1973**, *42*, 95. (b) Tomasi, J.; Mennucci, B.; Cammi, M. *Molecular Electrostatic Potentials: Concepts and Applications*; Murray, J. S., Sen, K. D., Eds.; Elsevier: Amsterdam, 1996.

(19) (a) Politzer, P.; Thruhlar, D. G. *Chemical Applications of Atomic and Molecular Electrostatic Potential*; Plenum: New York, 1981. (b) Murray, J. S.; Sen, K. D. *Molecular Electrostatic Potentials: Concepts and Applications*, Murray, J. S., Sen, K. D., Eds.; Elsevier: Amsterdam, 1996.

(20) (a) Gadre, S. R.; Shirsat, R. N. *Electrostatics of Atoms and Molecules*; Universities Press: Hyderabad, 2000. (b) Gadre, S. R. *Computational Chemistry: Reviews of Current Trends* Lesczynski, J. Ed.; World Scientific: Singapore, 2000; Vol. 4, and the references therein.

(21) (a) Pathak, R. K.; Gadre, S. R. *Proc. Indian Acad. Sci., Chem. Sci.* **1990**, *102*, 189. (b) Gadre, S. R.; Pathak, R. K. *J. Chem. Phys.* **1990**, *93*, 1170.

(22) (a) Pingale, S. S.; Gadre, S. R.; Bartolotti, L. J. *J. Phys. Chem. A* **1998**, *102*, 9987. (b) Gadre, S. R.; Bhadane, P. K. **1999**, *103*, 3512. (c) Gadre, S. R.; Babu, K.; Rendell, A. P. *J. Phys. Chem A* **2000**, *104*, 8976. (d) Suresh, C. H.; Koga, N.; Gadre, S. R. *J. Org. Chem.* **2001**, *66*, 6883. (e) Kulkarni, A. D.; Babu, K.; Gadre, S. R.; Bartolotti, L. J. *J. Phys. Chem. A.* **2004**, *108*, 2492. (f) Gadre, S. R.; Kulkarni, A. D. *Indian J. Chem.* **2001**, *39A*, 50.

(23) Frisch, M. J.; Trucks, G. W.; Schlegel, H. B.; Scuseria, G. E.; Robb, M. A.; Cheeseman, J. R.; Montgomery, J. A., Jr.; Vreven, T.; Kudin, K. N.; Burant, J. C.; Millam, J. M.; Iyengar, S. S.; Tomasi, J.; Barone, V.; Mennucci, B.; Cossi, M.; Scalmani, G.; Rega, N.; Petersson, G. A.; Nakatsuji, H.; Hada, M.; Ehara, M.; Toyota, K.; Fukuda, R.; Hasegawa, J.; Ishida, M.; Nakajima, T.; Honda, Y.; Kitao, O.; Nakai, H.; Klene, M.; Li, X.; Knox, J. E.; Hratchian, H. P.; Cross, J. B.; Bakken, V.; Adamo, C.; Jaramillo, J.; Gomperts, R.; Stratmann, R. E.; Yazyev, O.; Austin, A. J.; Cammi, R.; Pomelli, C.; Ochterski, J. W.; Ayala, P. Y.; Morokuma, K.; Voth, G. A.; Salvador, P.; Dannenberg, J. J.; Zakrzewski, V. G.; Dapprich, S.; Daniels, A. D.; Strain, M. C.; Farkas, O.; Malick, D. K.; Rabuck, A. D.; Raghavachari, K.; Foresman, J. B.; Ortiz, J. V.; Cui, Q.; Baboul, A. G.; Clifford, S.; Cioslowski, J.; Stefanov, B. B.; Liu, G.; Liashenko, A.; Piskorz, P.; Komaromi, I.; Martin, R. L.; Fox, D. J.; Keith, T.; Al-Laham, M. A.; Peng, C. Y.; Nanayakkara, A.; Challacombe, M.; Gill, P. M. W.; Johnson, B.; Chen, W.; Wong, M. W.; Gonzalez, C.; Pople, J. A. *Gaussian Devlopment Version*; Gaussian, Inc.: Wallingford, CT, 2004.

(24) (a) Cramer, C. J. *Essentials of Computational Chemistry*; Wiley: Chichester, 2002. (b) Rablen, P. R.; Lockman, J. W.; Jorgensen, W. L. *J. Phys. Chem. A* **1998**, *102*, 3782. (c) Estrin, D. A.; Paglieri, L.; Corongiu, G.; Clementi, E. *J. Phys. Chem.* **1996**, *100*, 8701. (d) Szczepaniak, K.; Szczesniak, M.; Person, W. B. *J. Phys. Chem. A* **2000**, *104*, 3852. (e) Thakkar, A. J.; Kassimi, N. E.; Hu, S. *Chem. Phys. Lett.* **2004**, *387*, 142.

(25) Dreuw, A.; Head-Gordon, M. *Chem. Rev.* **2005**, *105*, 4009.

(26) Mennucci, B. *J. Am. Chem. Soc.* **2001**, *124*, 1506.

(27) (a) Shukla, M. K.; Lesczynski, J. *J. Phys. Chem. A* **2002**, *106*, 11338. (b) Shukla, M. K.; Lesczynski, J. *J. Phys. Chem. A* **2003**, *107*, 5538. (c) Shukla, M. K.; Lesczynski, J. *J. Phys. Chem. B* **2005**, *109*, 17333. and the references therein. (d) Shukla, M. K.; Lesczynski, J. *J. Phys. Chem. A.* **2003**, *107*, 5538.

(28) Becke, A. D. *Phys. Rev. A: At., Mol., Opt. Phys.* **1998**, *38*, 3098.

(29) Lee, C.; Yang, W.; Parr, R. G. *Phys. Rev. B: Condens. Matter Mater. Phys.* **1988**, *37*, 785.

(30) Stratmann, R. E.; Scuseria, G. E.; Frisch, M. J. *J. Chem. Phys.* **1998**, *109*, 8218.

(31) (a) Bauernschmtt, R.; Alhrichs, R. *Chem. Phys. Lett.* **1996**, *256*, 454. (b) Casida, M. E.; Jamorski, C.; Casida, K. C.; Salahub, D. R. *J. Chem. Phys.* **1998**, *108*, 4439.

(32) Gview: A graphical user interface for Gaussian 03. More information may be found at http://www.gaussian.com/gv_plat.htm (accessed Nov. 15, 2007).

(33) (a) Cancès, E.; Mennucci, B.; Tomasi, J. *J. Chem. Phys.* **1997**, *107*, 3032. (b) Cancès, E.; Mennucci, B. *J. Math. Chem.* **1998**, *23*, 309. (c) Mennucci, B.; Cancès, E.; Tomasi, J. *J. Phys. Chem. B* **1997**, *101*, 10506.

(34) (a) Miertus, S.; Scrocco, E.; Tomasi, J. *Chem. Phys.* **1981**, *55*, 117. (b) Miertus, S.; Tomasi, J. *Chem. Phys.* **1982**, *65*, 239. (d) Cossi, M.; Barone, V.; Cammi, R.; Tomasi, J. *Chem. Phys. Lett.* **1996**, *255*, 327. (e) Barone, V.; Cossi, M.; Tomasi, J. *J. Chem. Phys.* **1997**, *107*, 3210. (f) Cossi, M.; Barone, V.; Mennucci, B.; Tomasi, J. *Chem. Phys. Lett.* **1998**, *286*, 253. (g) Barone, V.; Cossi, M.; Tomasi, J. *J. Comput. Chem.* **1998**, *109*, 404. (h) Mennucci, B.; Tomasi, J. *J. Chem. Phys.* **1997**, *106*, 5151.

(35) Cammi, R.; Mennucci, B.; Tomasi, J. *J. Phys. Chem. A* **2000**, *104*, 5631.

(36) Scalmani, G.; Frisch, M. J.; Mennucci, B.; Tomasi, J.; Cammi, R.; Barone, V. *J. Chem. Phys.* **2006**, *124*, 094107.

(37) *UNIPROP*, a molecular property calculation package; Theoretical Chemistry Group, Department of Chemistry, University of Pune: Pune, India. Bapat, S. V.; Shirsat, R. N.; Gadre, S. R. *Chem. Phys. Lett.* **1992**, *200*, 373.

(38) *Univis-2000*, see: Limaye, A. C.; Gadre, S. R. *Curr. Sci. (India)* **2001**, *80*, 1296.

(39) (a) Clouthier, D. J.; Ramsey, D. A. *Annu. Rev. Phys. Chem.* **1983**, *34*, 31. (b) Robin, M. B. *Higher Excited States of Polyatomic Molecules*; Academic Press: New York, 1985; *Vol. III*. (c) Walzl, K. N.; Koerting, C. F.; Kuppermann, A. *J. Chem. Phys.* **1987**, *87*, 3796.

(40) (a) Hosoya, H.; Tanaka, J.; Nagakura, S. *Bull. Chem. Soc. Jpn.* **1960**, *33*, 850. (b) Janssen, M. J. *Recl. Trav. Chim. Pays-Bas* **1960**, *79*, 454. (c) Rang, K.; Sandstrom, J.; Svensson, C. *Can. J. Chem.* **1998**, *76*, 811.

(41) (a) Bonaccorsi, R.; Scrocco, E.; Tomasi, J. *Jerusalem Symposia vol 6: Chemical and Biochemical Reactivity*; Pullman, B., Bergman, E., Eds.; Israeli Academy of Science: Jerusalem, 1974; p 387. (b) Cimiraglia, R.; Tomasi, J. *J. Am. Chem. Soc.* **1977**, *99*, 1135. (c) Daudel, R.; Le Rouzo, H.; Cimiraglia, R.; Tomasi, J. *Int. J. Quantum Chem.* **1978**, *13*, 537.

CT7002429